Received: 12 April 2022 | Revised: 30 June 2022 | Accepted: 2 July 2022

DOI: 10.1111/mmi.14963

RESEARCH ARTICLE

WILEY

Mycoplasma hyopneumoniae membrane protein Mhp271 interacts with host UPR protein GRP78 to facilitate infection

Qiao Pan | Qingyuan Xu | Tong Liu | Yujuan Zhang | Jiuqing Xin

State Key Laboratory of Veterinary Biotechnology, Harbin Veterinary Research Institute, Chinese Academy of Agricultural Sciences, Harbin, China

Correspondence
Jiuqing Xin, State Key Laboratory of Veterinary Biotechnology, Harbin Veterinary Research Institute, Chinese Academy of Agricultural Sciences, Harbin, China.
Email: xinjiuqing@caas.cn

Abstract

The unfolded protein response (UPR) plays a crucial role in *Mycoplasma hyopneumoniae* (*M. hyopneumoniae*) pathogenesis. We previously demonstrated that *M. hyopneumoniae* interferes with the host UPR to foster bacterial adhesion and infection. However, the underlying molecular mechanism of this UPR modulation is unclear. Here, we report that *M. hyopneumoniae* membrane protein Mhp271 interacts with host GRP78, a master regulator of UPR localized to the porcine tracheal epithelial cells (PTECs) surface. The interaction of Mhp271 with GRP78 reduces the porcine beta-defensin 2 (PBD-2) production, thereby facilitating *M. hyopneumoniae* adherence and infection. Furthermore, the R1-2 repeat region of Mhp271 is crucial for GRP78 binding and the regulation of PBD-2 expression. Intriguingly, a coimmunoprecipitation (Co-IP) assay and molecular docking prediction indicated that the ATP, rather than the substrate-binding domain of GRP78, is targeted by Mhp271 R1-2. Overall, our findings identify host GRP78 as a target for *M. hyopneumoniae* Mhp271 modulating the host UPR to facilitate *M. hyopneumoniae* adherence and infection.

KEYWORDS
a nucleotide-binding domain (NBD), GRP78, infection, Mhp271, *Mycoplasma hyopneumoniae*, protein–protein interaction, R1 repeats region, unfolded protein response

1 | INTRODUCTION

Porcine enzootic pneumonia (PEP) is caused by *Mycoplasma hyopneumoniae* (*M. hyopneumoniae*), which is characterized by dry coughing, severe respiratory distress, and growth reduction (Clampitt et al., 2021; Maes et al., 2018). This infection is highly prevalent, ranging between 38% and 100% in almost all areas of pig production worldwide, and causes significant economic losses (Maes, Sibila, et al., 2021).

M. hyopneumoniae is mostly believed to be an extracellular pathogen, which requires adherence to the host epithelium, mediated by adhesins, to establish infection (Leal Zimmer et al., 2020). Detailed characterization of these adhesins and their functional domains is necessary for us to better understand *M. hyopneumoniae*–host interactions. The P97 adhesin family is crucial for *M. hyopneumoniae* adhesion to the host and actively regulates the host natural immune response to promote *M. hyopneumoniae* survival (Berry et al., 2017; Deutscher et al., 2012; Jarocki et al., 2019; Maes, Boyen, et al., 2021; Raymond et al., 2018b). P97 has received the most attention in the P97 adhesin family due to its special repeat regions 1 and 2 (R1 and R2). It has been demonstrated that the R1 repeats region for P97 with a number varying from 9 to 15 of the R1 repeating

Qiao Pan and Qingyuan Xu contributed equally to this study.

units (sequence AAKPV[E]) is essential for its host binding (Clampitt et al., 2021; Hsu & Minion, 1998; Minion et al., 2000). Mhp271, a paralog of P97, is the only other *M. hyopneumoniae* protein containing R1 and R2 repeats associated with the adhesion process (Deutscher et al., 2010). Unlike P97, Mhp271 contains two R1 repeat regions (designated as R1-1 and R1-2): R1-1 region with three R1 repeating units exhibiting little sequence variation and R1-2 region with the number of R1 repeating units ranging from three to eight (Deutscher et al., 2010). It is worth mentioning that a minimum of eight R1 repeating units are required for tracheal cilia binding, suggesting that the repeating unit number of most Mhp271 R1 regions is not sufficient to adhere to host cilia (Minion et al., 2000). However, the fact is that the Mhp271 R1-2 region (which has six repeating units) can bind to host cilia with the help of the nearby R2 region (Deutscher et al., 2010). The adhesion function of the R1 region is complex, and it is interesting that this reduced number of repeat units in the R1 region still retains its adhesion function. To date, the functional and biological implications of the reduced number of repeating units in the R1 region of Mhp271 are poorly investigated.

Many factors, such as bacterial infection, ischemia, hypoxia, heat shock, and increased protein synthesis, impair endoplasmic reticulum (ER) functions, resulting in ER stress and evoking adaptive unfolded protein response (UPR) programs (Hetz et al., 2015). The UPR is a cytoprotective signaling pathway aimed at restoring cellular homeostasis that also invokes innate immune signaling in response to invading microorganisms (Celli & Tsolis, 2015; Mori, 2000). Thus, the UPR is important for host–pathogen interactions (Alshareef et al., 2021; Hotamisligil, 2010). GRP78, the initiation point/hallmark protein of the UPR, is an ER chaperone belonging to the heat shock protein 70 (HSP70) family. GRP78 has attracted attention for its critical role in the UPR (Wang et al., 2017). Despite its participation in ER-related functions, GRP78 is also detected in other cellular fractions, including mitochondria, nucleus, cytosol, and plasma membrane (Gonzalez-Gronow et al., 2009). In recent years, accumulating evidence indicates that many pathogens target GRP78 at the mammalian cell surface, modulating the host UPR to benefit their entry/replication (Ibrahim et al., 2019). For instance, GRP78 is employed by Coxsackievirus, Dengue virus serotype 2, Borna disease virus, and Japanese encephalitis virus for host entry; by classical swine fever virus (CSFV) and Ebola for their replication; and by *Rhizopus oryzae* for fungal invasion of the host endothelium (Chengcheng et al., 2020; Elfiky, 2020; Honda et al., 2009; Jindadamrongwech et al., 2004; Liu et al., 2010; Nain et al., 2017; Triantafilou et al., 2002). Regardless, whether GRP78 also serves as a target for *M. hyopneumoniae* to regulate the host UPR, and thus the bacterial adherence and infection have yet to be addressed.

Our previous work identified that *M. hyopneumoniae* blocks the unfolded protein response (UPR) to facilitate epithelial adhesion and infection (Pan et al., 2020). To gain a more mechanistic understanding of the *M. hyopneumoniae*–UPR interaction and how it is regulated, we investigated the *M. hyopneumoniae* proteins involved in the UPR regulation of *M. hyopneumoniae* and the potential role that host GRP78 may play. Here we demonstrate that the *M. hyopneumoniae* membrane protein Mhp271 interacts with GRP78 to modulate the host UPR and bacterial adherence and infection. We further identified that the R1-2 region of Mhp271 is critical for binding the N-terminal ATP-binding domain of GRP78. Thus, our data reveal a novel role of GRP78 in *M. hyopneumoniae* infection, highlighting the multiple roles of Mhp271 R1 repeats in the host–*M. hyopneumoniae* interaction, which may aid the development of novel *M. hyopneumoniae* therapeutics.

2 | RESULTS

2.1 | *M. hyopneumoniae* LAMPs inhibit the host UPR

Our previous study demonstrated that *M. hyopneumoniae* inhibits the host UPR, playing a key role in host pathogenesis (Pan et al., 2020). The mechanism underlying this UPR inhibition is unclear. We suspected that *M. hyopneumoniae* lipid-associated membrane proteins (LAMPs) have a role in UPR inhibition. Interactions of the *M. hyopneumoniae* LAMPs with the host cells are thought to be one of the major factors in mycoplasma pathogenesis (Shimizu et al., 2005). Thus, we treated the porcine tracheal epithelial cells (PTECs) with purified LAMPs or tunicamycin (Tu) or both (Figure 1a,b). As expected, Tu, a routinely used UPR inducer, significantly upregulated the expression of GRP78, a hallmark protein of the UPR (Figure 1b,c). Interestingly, Tu-induced upregulation of GRP78 in the PTECs was alleviated by the pretreatment with the purified LAMPs (Figure 1b,c). Additionally, no significant cytotoxicity was observed in LAMPs and Tu treatment (Figure 1d). These data suggest that one or more components of *M. hyopneumoniae* LAMPs interfere with the host UPR pathway.

2.2 | Mhp271 in *M. hyopneumoniae* LAMPs inhibits the host UPR

GRP78 is located on the cell surface of various mammalian cell types and is a target of pathogens for host UPR modulation (Chu et al., 2018; Honda et al., 2009; Nain et al., 2017; Triantafilou et al., 2002). Given that the LAMPs inhibit the UPR, we hypothesized that GRP78 of the PTECs is also a target of *M. hyopneumoniae* LAMPs. We first confirmed the cell surface expression of GRP78 in PTECs by flow cytometry analysis (Figure 2a,b). We then transfected PTECs with an HA epitope-tagged GRP78 and incubated with *M. hyopneumoniae* LAMPs. GRP78-binding proteins were eluted and silver stained. Protein bands unique to the LAMPs stimulation cells but not present in the control cells (transfected with GRP78-HA without LAMPs treatment) were excised and analyzed by protein mass spectrometry (MS) (Figure 2c). Mhp271 was identified with an approximate molecular weight of 118 kDa. The amino acid sequence of Mhp271 is shown in Figure S1, together with seven matched peptides detected in the MS analysis (highlighted in red).

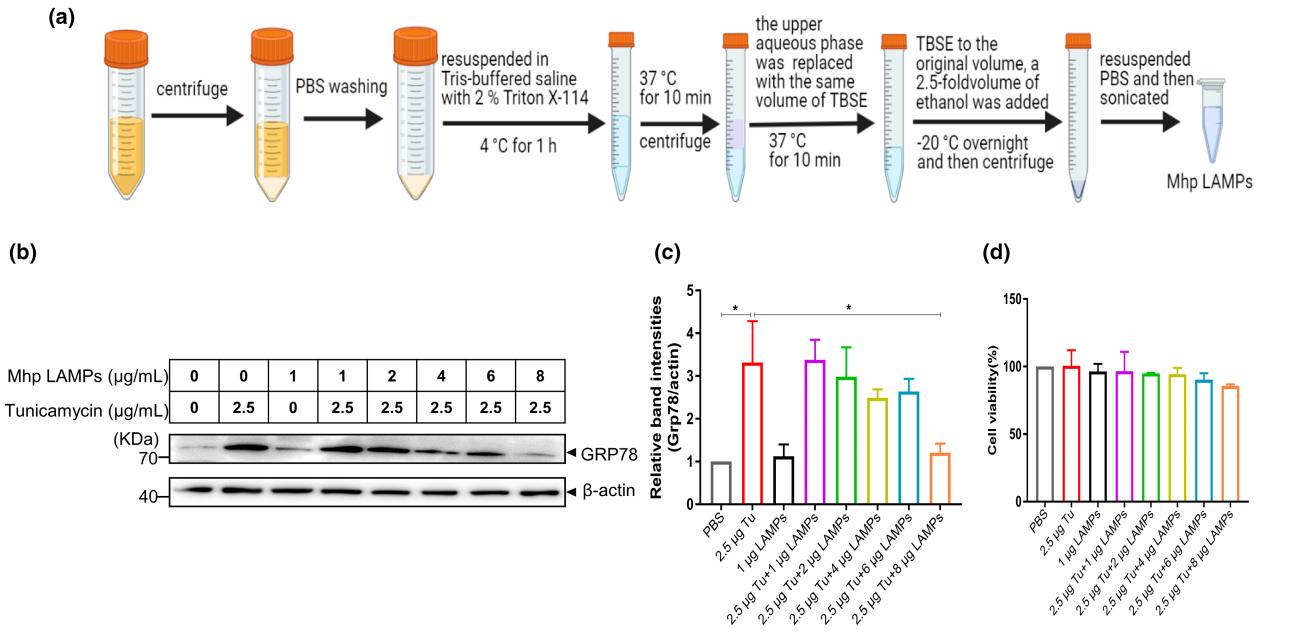

FIGURE 1 *M. hyopneumoniae* LAMPs inhibit the host UPR. (a) The pipeline of *M. hyopneumoniae* LAMPs extraction. (b and c) PTECs were stimulated by *M. hyopneumoniae* LAMPs (0, 1, 2, 4, 6, and 8 μg/ml) for 6 h, followed by the incubation of 2.5 μg/ml tunicamycin (Tu) for 6 h. The GRP78 level was quantified by Western blotting. The data were normalized to the corresponding values in PBS-treated cells. (d) LAMPs and/or Tu had no effects on the cell viability. All data are presented as the means ± *SD*s from three independent experiments, and significance was assessed by one-way ANOVA with Tukey's multiple comparison test. $^*p < .05$.

We next examined whether *M. hyopneumoniae* Mhp271 alone could mediate the GRP78 downregulation. We generated a soluble form of MBP-tagged Mhp271 fusion protein in *Escherichia coli* (*E. coli*) (Figure 2d). We treated PTECs with the purified Mhp271 fusion protein at different concentrations (Figure 2e,f). Mhp271 decreased the host GRP78 protein production in a dose-dependent manner with no apparent cytotoxicity (Figure 2g).

Thus, these results suggest that the *M. hyopneumoniae* membrane protein Mhp271 is a component of the host UPR GRP78 protein complex triggering the GRP78 degradation.

2.3 | Mhp271 directly interacts with the host GRP78

To further confirm the specific interaction between Mhp271 and GRP78, we performed a coimmunoprecipitation (Co-IP) analysis. HEK293T cells were cotransfected with plasmids expressing Flag-tagged Mhp271 and Myc-tagged GRP78 together or alone. Reciprocal interactions were observed using either anti-Flag or anti-Myc-tagged antibodies to conduct IP (Figure 3a,b).

To examine whether the interaction between Mhp271 and GRP78 was physically direct, we expressed and purified C-terminal glutathione-S-transferase (GST)-fused GRP78 protein and performed Far-Western blotting analysis on Mhp271-MBP-immobilized immunoblots (Figure 3c). A direct interaction was confirmed with the observation of the GRP78 band at the Mhp271-MBP position. Additionally, the subcellular localization of GRP78 and the Mhp271 protein complex in HEK293T cells was examined by confocal microscopy (Figure 3d). GRP78 was distributed in the cytoplasm and cytomembrane, and Mhp271 was distributed throughout the cytomembrane. GRP78 colocalized with Mhp271 on the cytomembrane.

Collectively, these findings suggest that the GRP78 protein is an interacting partner of the *M. hyopneumoniae* Mhp271 protein.

2.4 | The R1-2 region of Mhp271 is required for its interaction with the host GRP78

To define the key domain in Mhp271 determining the interaction with the host GRP78 protein, we generated truncated Mhp271 constructs with a Flag-tag at their C-terminus: Mhp271a, Mhp271b, and Mhp271c (Figure 4a). The three constructs were individually cotransfected with GRP78-Myc into HEK293T cells, and cell lysates were subjected to Co-IP assays. All three truncated constructs of Mhp271 were well expressed (Figure 4b,c), and only the Mhp271c (aa 703–1052) coimmunoprecipitated with the GRP78 protein (Figure 4b). The reverse Co-IP assay using beads conjugated with mAbs against Myc confirmed that GRP78 only interacted with the Mhp271c protein (Figure 4c). These data illustrate that the C-terminus of Mhp271, namely, aa 703–1052, is required for the interaction of Mhp271 with the GRP78 protein.

Subsequently, we analyzed the aa sequence of Mhp271c using the InterPro at EMBL-EBI (Apweiler et al., 2001) and SMART (Schultz et al., 1998). The prediction of the InterPro database showed that

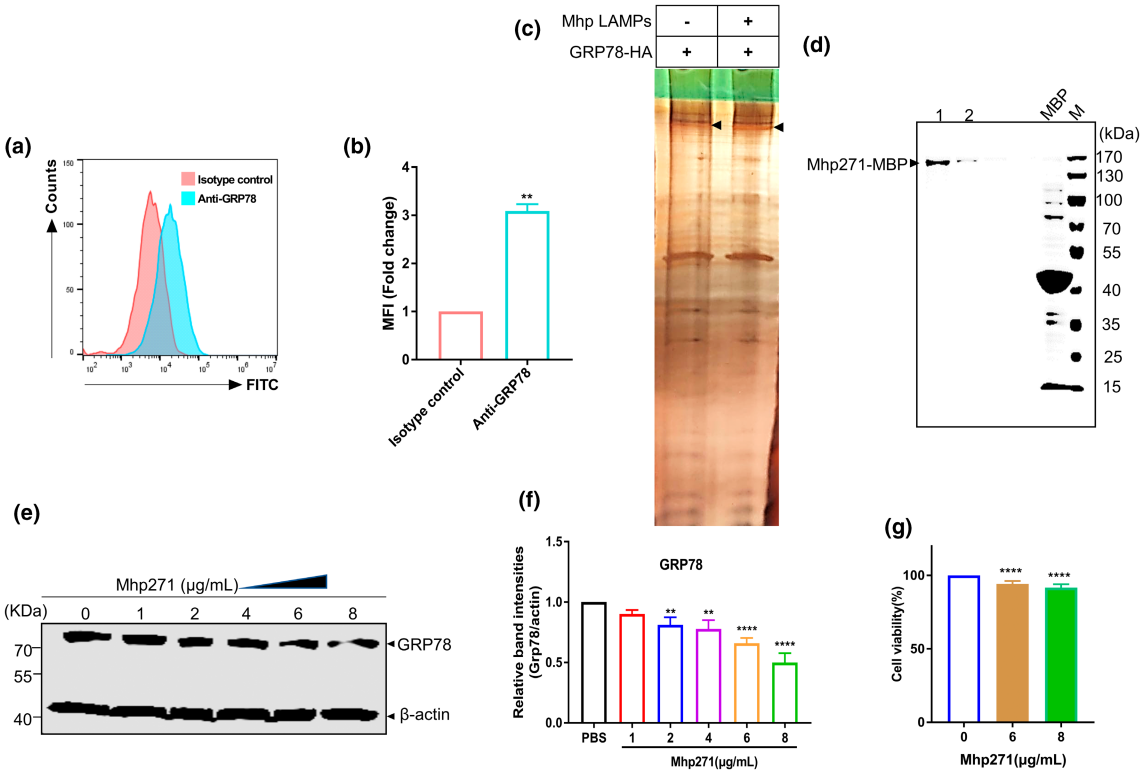

FIGURE 2 Mhp271 in *M. hyopneumoniae* LAMPs inhibits the host UPR. (a and b) GRP78 is exposed to the surface of PTECs. The cells were stained with anti-GRP78 antibody or isotype IgG and then incubated with secondary antibodies and followed by flow cytometric analysis of 5000 cells per sample (a). The MFI of GRP78 on the cell surface was quantified with isotype staining included as a control (b). (c) PTECs were transfected with GRP78-HA for 36 h and further incubated with 8 μg/ml *M. hyopneumoniae* LAMPs for 12 h. Whole-cell lysates (WCLs) were applied to anti-HA magnetic beads. GRP78 and interacting proteins were eluted, separated by SDS-PAGE, and silver-stained. (d) The purified Mhp271–MBP protein was identified by SDS-PAGE. The Mhp271–MBP fusion protein is indicated by the arrow. (e and f) The GRP78 level was downregulated following the Mhp271–MBP protein incubation in PTECs demonstrated by Western blotting (e). The data were normalized to the corresponding values in untreated cells (f). (g) Cell viability in PTECs treated with 6 or 8 μg/ml Mhp271–MBP was slightly decreased. The data are presented as the means ± *SD*s from three independent experiments, and significance was assessed by two-tailed Student's *t* test (b) or by one-way ANOVA with Dunnett's multiple comparison test relative to the control (f and g). $^{**}p < .01$; $^{****}p < .0001$.

Mhp271c encodes a 350-aa protein consisting of three domains: aa 795–830, 907–944, and 990–1032. SMART predicted Mhp271c containing two domains: aa 808–831 and 998–1034. Based on the predictions of the two databases, aa 808–830 and 998–1032 may be the key domains interacting with host molecules. Interestingly, we found that the two domains overlap with the two R1 repeat regions of Mhp271 (aa 802–820 and 999–1027, designated as R1-1 and R1-2 separately). An R2 repeat region (aa 916–935) is located between the two R1 regions (Figure 4d). The R1 comprises tandem pentapeptide repeats with the sequence AAKPV(E), whereas R2 comprises tandem decapeptide repeats with the sequence GTPNQGKKAE (Hsu et al., 1997). For a better understanding of the three regions, the structure of Mhp271 protein was predicted using I-TASSER (Zhang, 2008). The most accurate model predicted by I-TASSER was selected based on C-score, ERRAT, and verify-3D. As shown in Figure 4e, the three repeat regions were present on the surface of this 3D structure.

Next, we confirmed the role of the two R1 regions of Mhp271 in interacting with host GRP78. Due to the unclear function for the R2 repeats region, we also assessed its role in this interaction. To do this, the Mhp271c partial deletion plasmid lacking the R1-1, R1-2, or R2 region was individually cotransfected with GRP78-Myc into HEK293T cells and cell lysates at 36 h posttransfection were subjected to a Co-IP assay (Figure 4f). The results showed that the absence of the R1-2 region eliminated the ability of Mhp271c to interact with the GRP78 protein, which is consistent with the results of domain prediction by the two databases, suggesting that the R1-2 region (aa 999–1027) in Mhp271 is critical for the interaction with the GRP78 protein. A Far-Western blotting analysis was then performed to directly verify that Mhp271 R1-2 protein could bind to GST-fused GRP78 protein (Figure 4g).

Taken together, these data suggest that the R1-2 region of Mhp271 is necessary and sufficient for the interaction with host GRP78.

2.5 | Mhp271 plays an important role in *M. hyopneumoniae* infection of PTECs

Considering that the UPR positively regulates the PBD-2 release, we first asked whether Mhp271 impairs the PBD-2 production by

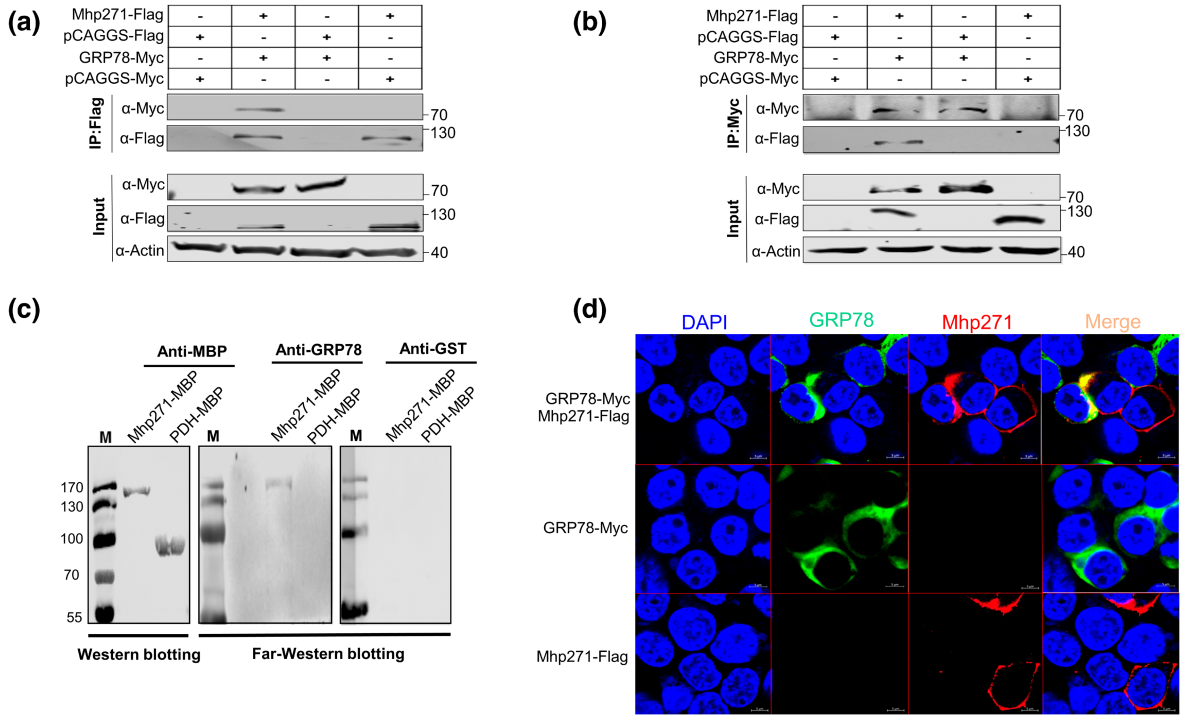

FIGURE 3 Mhp271 directly interacts with the host GRP78. (a and b) Mhp271-Flag coimmunoprecipitated with GRP78-Myc. HEK293T cells were transfected with Mhp271-Flag or GRP78-Myc, or the control plasmids pCAGGS-Flag or pCAGGS-Myc for 36 h. Cell lysates were collected for Co-IP with beads conjugated with anti-Flag antibody (a) and Myc antibody (b). (c) Far-Western blotting analysis showed the binding of GRP78 with the Mhp271 protein. The proteins Mhp271-MBP and PDH-MBP (negative control) were transferred onto nitrocellulose (NC) membranes. Left: The NC membrane was incubated with anti-MBP antibodies; middle: The NC membrane was first incubated with the GRP78-GST protein and then with anti-GRP78 antibodies; right: The NC membrane was first incubated with the GST protein and then with anti-GST antibodies. (d) Colocalization of the Mhp271 and GRP78 proteins. HEK293T cells were transfected with GRP78-Myc, Mhp271-Flag, or both. Cells were subjected to indirect immunofluorescence to detect GRP78-Myc (green) and Mhp271-Flag (red) with mouse anti-Myc and rabbit anti-Flag antibodies, respectively. The position of the nucleus is indicated by DAPI (blue) staining in the merged image. Scale bars = 5 μm. Experiments were performed at least three times.

causing host GRP78 degradation (Pan et al., 2020). Thus, we checked host PBD-2 production in PTECs postincubation with Mhp271 protein or transfection with Mhp271c/Mhp271c(ΔR1-2) plasmids. As shown in Figure 5a, host PBD-2 production in PTECs was reduced by the addition of 6 or 8 μg/ml Mhp271. A similar result was obtained in PTECs transfected with Mhp271c-Flag, while the PBD-2 production in PTECs transfected with Mhp271c(ΔR1-2)-Flag was almost unchanged (Figure 5b). The data indicated that Mhp271 or Mhp271c decreases host PBD-2 production by triggering GRP78 degradation.

PBD-2 has been proven to suppress *M. hyopneumoniae* adherence in PTECs, we next investigated whether the PBD-2 inhibition by Mhp271 facilitates *M. hyopneumoniae* adherence. After PTECs were treated as described above, TaqMan quantitative PCR (qPCR) was performed and showed that the stimulation with Mhp271 at 6 or 8 μg/ml increased the *M. hyopneumoniae* number adhered to PTECs (Figure 5c), as well in PTECs transfected with Mhp271c-Flag (Figure 5d). However, the *M. hyopneumoniae* number adhered to PTECs transfected with Mhp271c(ΔR1-2)-Flag was almost no alteration, in contrast to the PTECs transfected with the empty vector pCAGGS-Flag transfection (Figure 5d). These results were further confirmed by an immunofluorescence assay (IFA) (Figure 5e,f), suggesting that Mhp271 or Mhp271c benefits *M. hyopneumoniae* adhesion in PTECs. Therefore, these findings imply that Mhp271 or Mhp271c can suppress the PBD-2 production by inducing GRP78 degradation, thereby promoting *M. hyopneumoniae* adherence and infection to PTECs.

We further assessed whether Mhp271 elicits GRP78 degradation via its R1-2 region interacting with GRP78. A polyclonal antibody against the Mhp271 R1-2 region was prepared to block the interaction of Mhp271 R1-2 with GRP78, and 8 μg/ml Mhp271 protein were separately incubated with the polyclonal antibody against Mhp271 R1-2 region and negative serum before the addition to PTECs. The GRP78 level was evaluated by Western blotting assay (Figure 5g). We observed that the preincubation with the polyclonal antibody against Mhp271 R1-2, Mhp271 could not evoke host GRP78 degradation, suggesting that the GRP78 degradation by Mhp271 is likely occurring through the interaction of its R1-2 region with GRP78.

2.6 | The interaction with the Mhp271 R1-2 region requires the NBD of GRP78

The porcine GRP78 protein consists of a total of 654 aa residues including a nucleotide-binding domain (NBD, aa 125–280) and a

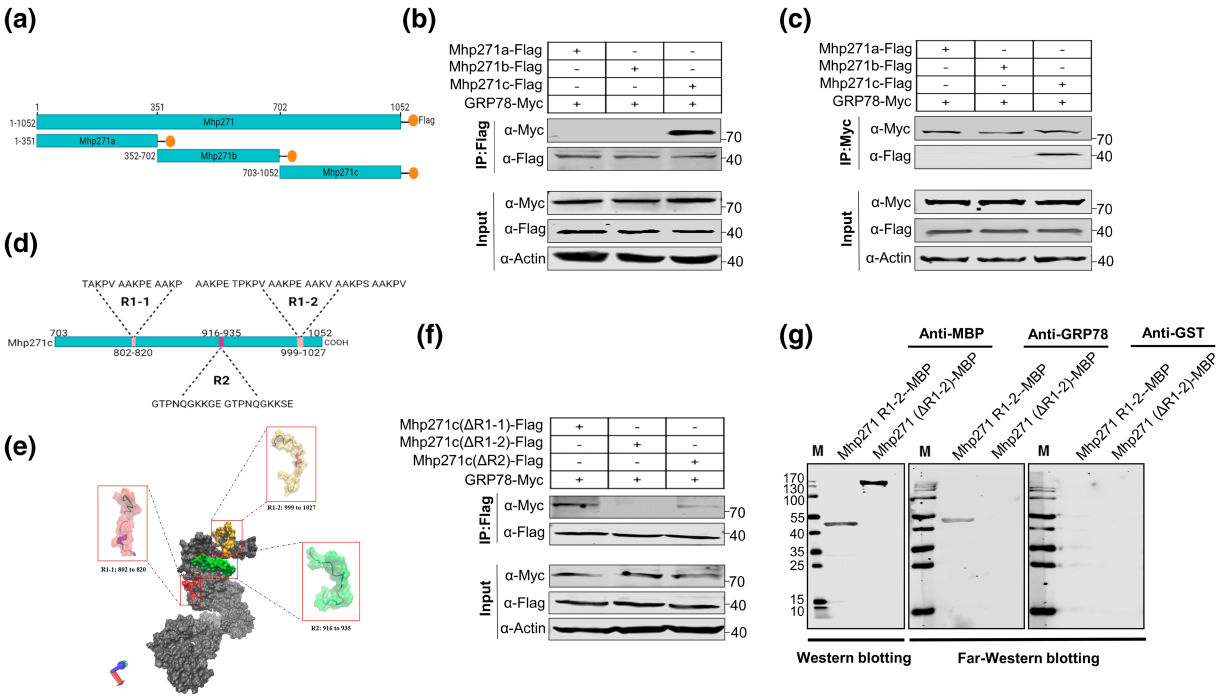

FIGURE 4 The R1-2 region of Mhp271 is necessary for the interaction with the host GRP78. (a–c) The fragment of Mhp271 aa 703–1052 interacted with the GRP78 protein. Schematic of the Mhp271 truncates tagged with Flag and locations of the aa residues are noted (a). HEK293T cells were cotransfected with GRP78-Myc and truncated Mhp271 constructs (Mhp271a-Flag, Mhp271b-Flag, and Mhp271c-Flag), and the cell lysates were collected for Co-IP assays using beads conjugated with anti-Flag antibody for Flag-tagged Mhp271 truncates (b) or with Myc antibody for Myc-tagged GRP78 (c). (d) Schematic of locations and aa sequences of the R1-1, R2, and R1-2 regions in Mhp271. (e) The PDB structure of Mhp271 was determined based on C-score, ERRAT, and verify-3D using I-TASSER. Full-length Mhp271 protein (gray) and its repeat regions are shown here in different colors. This structure was visualized in VMD software. (f) The Mhp271c plasmid lacking the R1-2 region did not immunoprecipitate with the GRP78. HEK293T cells were cotransfected with GRP78-Myc and the three deletion Mhp271c deletion constructs (Mhp271c(ΔR1-1), Mhp271c(ΔR1-2), and Mhp271c(ΔR2)). Cell lysates were collected for Co-IP assays using beads conjugated with anti-Flag antibodies. (g) Far-Western blotting analysis showed the binding of Mhp271 R1-2 with the GRP78 protein.

substrate-binding domain (SBD, aa 400–500). The NBD binds ATP while the SBD binds substrate peptide/protein in the form of an excluded segment or partially folded protein (Lee, 2014). We previously demonstrated that the R1-2 region of Mhp271 is necessary for its binding to the host GRP78, but it was unclear which domain of GRP78 is needed for the interaction with the Mhp271 R1-2 region. To address this question, we constructed the dominant-negative mutant plasmid G227D unable to bind ATP, the T453D mutant unable to bind protein substrates, and the R197H mutant, which renders GRP78 unable to associate with cochaperone DnaJ proteins (Figure 6a) (Tsai et al., 2015). Upon transfection of the mutant plasmids into 293T cells, a Co-IP assay was performed using an anti-Flag antibody to confirm the domain of GRP78 protein involved in the interaction with the Mhp271 R1-2. As shown in Figure 6b, GRP78-Myc, the T453D, and R197H mutant bound to the Mhp271 C-terminus, whereas the G227D mutant did not. The result suggested that the ATP-binding domain of GRP78 is necessary for the interaction with the Mhp271 R1-2 region.

Subsequently, we analyzed the binding site of GRP78 with Mhp271 R1-2 using some molecular modeling docking web servers to further understand the above result. A 3D model of porcine GRP78 was built using the SWISS-MODEL web server (Guex & Peitsch, 1997), with the human Hsp70 chaperone BiP (PDB ID: 5E84) as a template. The interaction interface between GRP78 and Mhp271 R1-2 was investigated with several docking methods. Ten models were predicted by ZDOCK docking server along with their expected confidence values (Pierce et al., 2014). Molecular docking analysis of these peptide-GRP78 complexes revealed that the Mhp271 R1-2 region is most likely to dock with the NBD of the GRP78 protein (Figure 6c). In addition, Vasker, an additional docking method was also used to survey the binding domain of GRP78 with Mhp271 R1-2 (Figure S2b) (Vakser, 2014). Similar results were obtained and suggested that the NBD of GRP78 protein plays a key role in the interaction with Mhp271 R1-2.

To further assess the contributions of Mhp271 to the host GRP78 reduction of *M. hyopneumoniae*, a specific antibody against Mhp271 was purified from murine serum anti-Mhp271 and demonstrated to block Mhp271-induced degradation of host GRP78 (Figure S2c). *M. hyopneumoniae* was pretreated with or without the purified antibody against Mhp271 and then incubated with PTECs. The GRP78 level was estimated by Western blotting assay (Figure 6d,e). We observed that the blockade of Mhp271 could not prevent *M. hyopneumoniae* from downregulating host GRP78 levels, indicating other mechanisms are also adopted by *M. hyopneumoniae* to reduce the host GRP78 content.

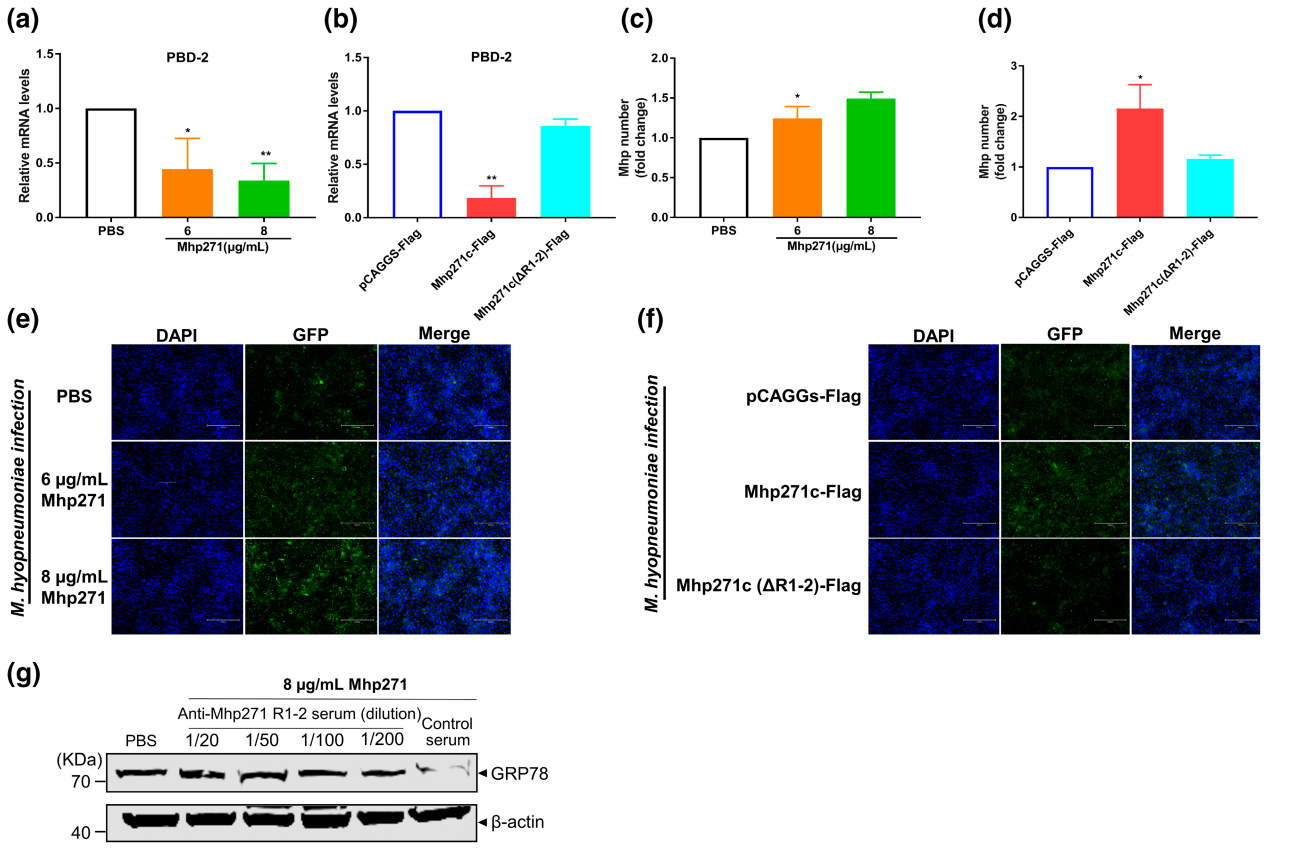

FIGURE 5 Mhp271 plays an important role in *M. hyopneumoniae* infection to PTECs. (a and b) Mhp271 downregulated host PBD-2 expression. PTECs were treated with PBS or the Mhp271 protein for 24 h (a) or transfected with pCAGGS-flag, Mhp271c-flag, or Mhp271c(ΔR1-2) for 36 h (b), and PBD-2 mRNA level was quantified by qPCR. (c–f) Mhp271 facilitated *M. hyopneumoniae* adherence to PTECs. PTECs were treated as described in panels A and B and then incubated with *M. hyopneumoniae* for 12 h. Cells were washed twice with PBS and harvested to analyze the number of *M. hyopneumoniae* cells adhered to PTECs by TaqMan qPCR (c and d), or cells were subjected to an *M. hyopneumoniae* P46 protein IFA with mouse anti-*M. hyopneumoniae* monoclonal antibody 3G11 (green) to detect *M. hyopneumoniae* adherence to PTECs. DAPI was used to stain cellular nuclei (blue) (e and f). Controls on uninfected cells with PBS or Mhp271 protein treatment or with pCAGGS-Flag, Mhp271c-Flag, or Mhp271c(ΔR1-2) transfection are shown in Figure S2a. (g) Murine serum against Mhp271 R1-2 prevented Mhp271 from triggering host GRP78 degradation in PTECs, and 8 μg/ml Mhp271 protein was incubated with murine serum against Mhp271 R1-2 (diluted 1:20, 1:50, 1:100, and 1:200) or negative murine serum (diluted 1:20) for 30 min and then added to PTECs. The GRP78 level in PTECs was determined by Western blotting. All assays were performed with three independent experiments, and values represent the means ± *SD*s. Significance was assessed by one-way ANOVA with Dunnett's multiple comparison test relative to the control. $^{*}p < .05$; $^{**}p < .01$.

3 | DISCUSSION

Interference with the host cell UPR during bacterial pathogens infection is an emerging theme in bacterial pathogenesis, as documented previously with viral pathogens (Pavio et al., 2003; Tardif et al., 2004). The ability of *M. hyopneumoniae* to inhibit UPR pathways has been documented recently, whereas the underlying molecular mechanism is unclear (Pan et al., 2020). In the present study, we demonstrated for the first time that *M. hyopneumoniae* utilizes its membrane protein Mhp271 to interact with UPR GRP78 and causes GRP78 degradation, thereby modulating host UPR to facilitate its adherence to and infection of the host cells.

GRP78 plays a central role in regulating the UPR to maintain the integrity of pivotal ER functions (Pfaffenbach & Lee, 2011; Zhu & Lee, 2015). GRP78 is localized to the ER membrane and involved in a wide range of physiological processes including protein folding and assembly, translocation of newly synthesized polypeptides, and degradation of misfolded proteins (Lee, 2014). Recent studies have shown that GRP78 is also present on the plasma membranes of many cell types such as HeLa cells and human monocyte-derived macrophages (Bellani et al., 2014; Bhattacharjee et al., 2005; Honda et al., 2009; Jindadamrongwech et al., 2004; Philippova et al., 2008; Triantafilou et al., 2002). Thus, GRP78 is a central component of UPR presenting on endo and plasma membrane surfaces, making it an ideal viral target (Broquet et al., 2007; Chen et al., 2010; Hirayama et al., 2004; Iordanskiy et al., 2004; Padwad et al., 2010; Surtees et al., 2016; Taguwa et al., 2015).

Indeed, mounting evidence suggests that viral pathogen proteins interact with the host GRP78 to regulate the host UPR/innate immune response for viral entry or replication. Bacteria-targeting

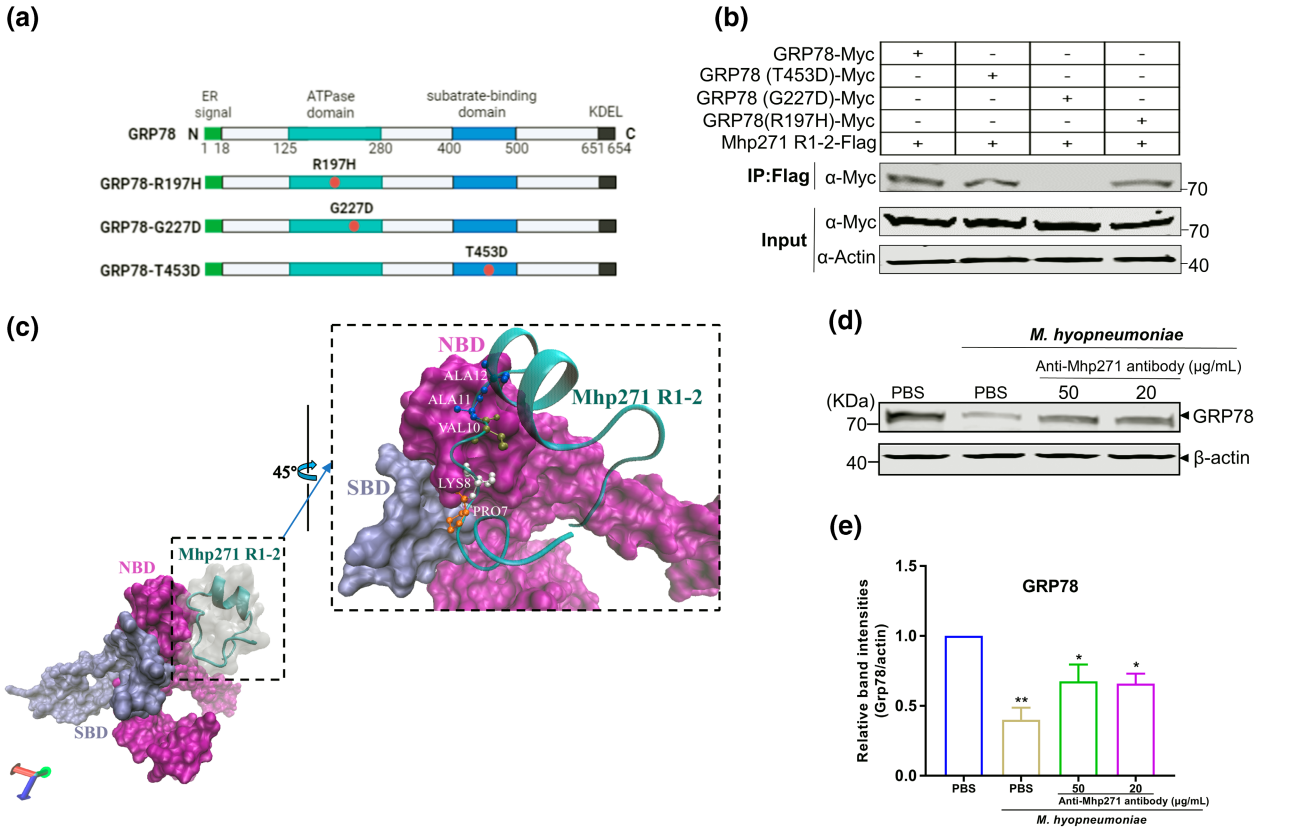

FIGURE 6 The interaction with Mhp271 requires the NBD of GRP78. (a) Schematic illustration of the indicated domains of GRP78 and Myc-tagged mutated forms of porcine GRP78 encoded by the expression plasmids. (b) The G227D mutant of GRP78-Myc was unable to coimmunoprecipitate with Mhp271 R1-2-Flag. GRP78-Myc or the indicated mutant forms of GRP78-Myc was cotransfected with Mhp271 R1-2-Flag into HEK293T cells. Cell lysates were collected for Co-IP with beads conjugated with anti-Flag antibodies. (c) The representative docking pose of the Mhp271 R1-2 with the swine GRP78 structure (PDB ID: 5E84) was achieved using the ZDOCK web server. ZDOCK predicted Mhp271 R1-2 binding with the NBD domain of GRP78. Colored surfaces represented the structures according to the domains. GRP78 nucleotide-binding domain (NBD) in purple, GRP78 substrate-binding domain (SBD) in iceblue. Both the silver surface and cyan cartoon represent Mhp271 R1-2. The aa residues from the Mhp271 R1-2 (cyan cartoon) which are close to the NBD of GRP78 (purple surface) are labeled and represented in colored sticks in the enlarged panel. The docking results of Mhp271 R1-2 with GRP78 were visualized in VMD software. (d and e) The block of Mhp271 could not prevent *M. hyopneumoniae* from reducing host GRP78 content. *M. hyopneumoniae* was incubated with the purified antibodies against Mhp271 (20 and 50 μg/ml) or PBS for 30 min and then added to PTECs. The GRP78 level in PTECs was determined by Western blotting. The data were normalized to the corresponding values in cells infected by negative serum incubated *M. hyopneumoniae* and represent the means ± *SD*s of the results from three independent experiments. Significance was assessed by one-way ANOVA with Dunnett's multiple comparison test relative to the control. $^{*}p < .05$; $^{**}p < .01$.

host GRP78 is very rarely reported, but it is beginning to emerge. Previous studies on *Brucella abortus* (*B. abortus*) showed that *B. abortus* adopts T4SS substrate VceC to interact with host GRP78 for ER stress induction, promoting its infection (de Jong et al., 2013). Likewise, Shiga-toxigenic *Escherichia coli* (*E. coli*) was reported to secrete an AB5 type toxin, Subtilase cytotoxin (SubAB), which interacts with and specifically cleaves GRP78 (Morinaga et al., 2008; Paton et al., 2006). Our research on *M. hyopneumoniae* provides additional evidence for bacterial targeting of the host GRP78. Given the critical role of GRP78 in microbial pathogenesis, this targeting of the host GRP78 may be an important mechanism in *M. hyopneumoniae* infection.

GRP78 is an essential heat shock protein (HSP) 70 resident protein in the endoplasmic reticulum that belongs to the ubiquitous molecular chaperones involved in many cellular processes. A large set of cochaperones comprising J-domain proteins and nucleotide exchange factors (NEFs) stimulate the ATPase activity of HSP70s, which is allosterically coupled to substrate binding and release (Kampinga & Craig, 2010). It is believed that the GRP78 C-terminus participates in protein binding, whereas the N-terminus acts as a regulatory domain governing binding through conformational changes of GRP78 (Jindadamrongwech et al., 2004). Microbial competitive binding to the N-terminal domain of host GRP78 regulates its ability to bind to substrates, thereby shaping GRP78's involvement in normal cellular processes, which becomes an important approach to modifying host immune response. Such cases have been reported with the Borna virus and Influenza A virus (Honda et al., 2009; Li et al., 2011). In the present study, we identified this host-GRP78 regulation of *M. hyopneumoniae*.

The P97/P102 paralog family on the surface of *M. hyopneumoniae* plays key roles in interactions with host cells,

extracellular matrix components, and circulating host proteins (Adams et al., 2005; Bogema et al., 2011; Bogema et al., 2012; Burnett et al., 2006; Deutscher et al., 2010; Seymour et al., 2012; Wilton et al., 2009). The multifunctional adhesins belonging to the P97/P102 family include Mhp182 (P102), Mhp183 (P97), Mhp493 (P159), Mhp494 (P216), Mhp683 (P135), Mhp271, Mhp107, and Mhp108 (P116) (Bogema et al., 2012). Characterization of these adhesins represented a major event in understanding the mechanisms of *M. hyopneumoniae* adherence, colonization, and pathogenesis (Leal Zimmer et al., 2020). In this study, in search of GRP78 interacting proteins in *M. hyopneumoniae* LAMPs, we performed MS analysis of the GRP78 immunoprecipitated complex and identified Mhp271. The interaction of Mhp271 with the host GRP78 is further confirmed through Co-IP assays, far WB, and laser confocal microscopy. To the best of our knowledge, this is the first report showing the interaction of Mhp271 with the host GRP78. However, we recognize our study's limitations. We are unable to validate this interaction in vivo due to the absence of an effective method for targeted mutations of the *M. hyopneumoniae* gene at present.

A previous study indicated that the Mhp271 C-terminus is capable of binding heparin, fibronectin, and porcine cilia, and two repeat regions in this sequence fragment have been identified as potential contributors (Deutscher et al., 2010). Indeed, repeating domains are common in bacterial proteins that engage in host–pathogen interactions and are essential for adhesion functions (e.g., *M. pneumoniae* P30 and *M. gallisepticum* PvpA; Boguslavsky et al., 2000; Dallo et al., 1996). Furthermore, the repeat regions in Mhp271 contain multiple proline residues, forming an extended structure and flexible stretch with strong binding capability. There are six well-known families of the proline-rich region (PRR)-binding modules: the SH3 domains, the WW domains, the EVH1 domains, the CD2-binding domains, the UEV domains, and the single-domain profilin proteins (Ball et al., 2005). Studies on group A *Streptococcus pyogenes* (GAS) identified bacterial GrpE, a part of the HSP70 chaperone complex (GrpE, DnaJ, and DnaK), also as a PRR protein-binding protein. Although GAS and human GrpE have 23% of the same amino acid sequence, they have a functionally conserved ATPase-binding site (Murakami et al., 2012). Some of the research on the interaction between antimicrobial peptides (AMPs) and HSPs further indicated that PRR AMPs can enter bacteria to inactivate the chaperone DnaK by binding to its ATPase domain (Cytryńska et al., 2020). Consistent with the results of these studies, our results showed that the PRR regions (R1 regions) in Mhp271 bind to the ATPase domain of host GRP78 (a member of the HSP70 family), which further emphasizes the multiple adhesion function of the C-terminus/the repeating regions in Mhp271.

The variable number of tandem repeat (VNTR) regions often involves protein–protein interactions (Hannan, 2018). *M. hyopneumoniae* P97 contains an R1 repeats region with a number varying from 9 to 15 of the R1 repeating units (sequence AAKPV(E)), which is essential for binding to tracheal cilia, heparin, and GAGs (Jenkins et al., 2006). Mhp271 as a paralog of P97 also has the R1 repeats region, but unlike P97, it contains two R1 repeat regions (designated as R1-1 and R1-2). Homologs from all strains displayed three R1 repeating units that exhibited little sequence variation within R1-1, whereas the number of R1 repeating units in R1-2 ranged from three to eight (Deutscher et al., 2010). The function and biological significance of this reduced number of R1 repeating units in Mhp271 R1 regions have not been fully determined. Previous studies suggested that a minimum of eight R1 repeating units are required for tracheal cilia binding, while three R1 repeating units are needed for antibody recognition (Minion et al., 2000). Despite a hypothesis that four or more R1 repeating units might provide effective adhesion in swine, it has never been verified (Minion et al., 2000). In this study, we confirmed that the R1-2 region of Mhp271 with six R1 repeating units (in *M. hyopneumoniae* strain 11) has the ability to bind to the host GRP78. Furthermore, the R1 repeats region adhesion is not totally determined by a strict repeat number requirement, as evidenced by the absence of P97 in our analysis of the GRP78 protein complex. It was likely that an excessive number of repeating units may partially bury the key sites of the R1 region interacting with GRP78, suggesting an important relation of the R1 repeats region adhesion with the 3D structure formed. This conclusion is consistent with a previous report that an R2 domain located near an R1 region with less than eight repeating units may function to assist in binding porcine cilia (Deutscher et al., 2010). Further study is necessary to ascertain the exact mechanism of the R1 repeats region binding to the host GRP78.

The interaction of adhesins with host molecules determines bacterial adherence and entry into host cells as well as its cellular and tissue tropism (Kirchner & Meyer, 2005). Although *M. hyopneumoniae* has historically been considered an extracellular pathogen, its entry into swine epithelial cells has recently been demonstrated, which is strengthened by the isolation of *M. hyopneumoniae* from the liver, spleen, kidneys, and bronchial lymph nodes of experimentally infected swine (Le Carrou et al., 2006; Raymond et al., 2018b). Clearly, the ability of *M. hyopneumoniae* to invade the respiratory or lung epithelial cells to target a wide range of tissues is being gradually recognized, although the detail of the mechanism needs further study. The interaction of *M. hyopneumoniae* with many different cellular proteins may explain the broad tissue tropism seen in *M. hyopneumoniae* infection (Martines et al., 2015). It is perhaps unsurprising that *M. hyopneumoniae* can interact with many cellular proteins, as illustrated by Raymond et al. who identified 105 PK-15 cell proteins using biotinylated *M. hyopneumoniae* surface proteins as bait for affinity chromatography. They further ascertained that actin exists in all eukaryote cells as an important receptor for *M. hyopneumoniae* and may facilitate a broad tissue tropism of *M. hyopneumoniae* (Raymond et al., 2018a). In our study, we confirmed GRP78 as an interaction target of *M. hyopneumoniae*, underlining the possibility of its broad tissue tropism, given that GRP78 is widely expressed on the surface of various human and animal cells.

In summary, we identified that *M. hyopneumoniae* Mhp271 can directly regulate host cell UPR to facilitate bacterial adherence and infection by interacting with host GRP78. Our findings improve our

understanding of the interaction between *M. hyopneumoniae* and the host, providing new insights into the molecular pathogenesis of *M. hyopneumoniae*. We hope that this and future studies may lead to the development of new therapies against diseases caused by *M. hyopneumoniae*.

4 | MATERIALS AND METHODS

4.1 | Mycoplasma strains, cells, and culture conditions

M. hyopneumoniae ATCC 25095 was purchased from the American Type Culture Collection (ATCC) and cultivated in a mycoplasma medium (Basal Media, Shanghai, China) at 37°C. To estimate the numbers of CFU in the cultures, serial dilutions were plated on a modified pleuropneumonia-like organism (PPLO) medium containing 1.5% agarose (V2111; Promega) and incubated at 37°C. CFU was counted 7–10 days later using a microscope (Vogl et al., 2008). *M. hyopneumoniae* was pelleted by centrifugation at 10,000*g* for 10 min and resuspended at 1.0×10^6 CFU/ml in phosphate buffered saline (PBS).

PTECs were prepared from the tracheas of two 5-week-old specific-pathogen-free (SPF) piglets using previously described protocols (Wang et al., 2018). Human embryonic kidney cells (HEK293T) were purchased from ATCC. PTECs and HEK293T cells were cultured in Dulbecco's modified Eagle's medium (DMEM) supplemented with 10% heat-inactivated fetal bovine serum (FBS), 1% antibiotics (100 μg/ml streptomycin and 100 U/ml penicillin; Gibco), and 10 mM HEPES (Invitrogen). The cells were incubated at 37°C in 5% CO_2.

4.2 | LAMPs preparation

LAMPs were prepared as described previously (He et al., 2009). Briefly, *M. hyopneumoniae* was cultivated in a mycoplasma medium until the beginning of the stationary growth phase (when a red pH indicator turned orange) and then collected by centrifugation. *M. hyopneumoniae* cells were washed with PBS twice and resuspended in 5 ml of Tris-buffered saline (TBS; 50 mM Tris-Cl, pH 8.0, 0.15 M NaCl) containing 1 mM EDTA (TBSE), to which Triton X-114 was added to a final concentration of 2% and incubated at 4°C for 1 h. The lysate was then incubated at 37°C for 10 min for phase separation. After centrifugation, the upper aqueous phase was removed and replaced with the same volume of TBSE. The solution was vortexed and incubated at 4°C for 10 min. The phase separation process was repeated twice. The final Triton X-114 phase was resuspended in TBSE to the original volume, and 2.5-fold volumes of ethanol were then added to precipitate the membrane components overnight at −20°C. After centrifugation, the pellet was resuspended in PBS and lysed by sonication. Protein concentrations were examined using the Bradford assay (Thermo Scientific, Waltham, MA, USA). The endotoxin concentration of the heat-inactivated mycoplasma LAMPs was <0.04 endotoxin units/ml, as checked by the Limulus amebocyte lysate assay (Associates of Cape Cod, Falmouth, MA, USA).

4.3 | Plasmids construction and transfection

The GRP78 gene was PCR amplified from PTECs and cloned into the pCAGGS-HA vector (Clontech) with the restriction enzymes *Kpn* I and *Xho* I.

The Flag-tag sequence was cloned into the expression plasmid pCAGGS at the C-terminus (Niwa et al., 1991). The Mhp271 gene (with *Bam* HI and *Sac* I sites) was codon-optimized and synthesized by the Beijing Genomics Institute (BGI, Beijing, China). This fragment was cloned into the pCAGGS-Flag vector. Three truncated Mhp271 constructs based on pCAGGS-FLAG were generated to express the aa 1–351, 352–702, and 703–1052 of Mhp271 and named Mhp271a-Flag, Mhp271b-Flag, and Mhp271c-Flag, respectively. The constructs based on Mhp271c-Flag with the R1-1, R2, or R1-2 region deleted were separately named Mhp271c(ΔR1-1)-Flag, Mhp271c(ΔR2)-Flag, and Mhp271c(ΔR1-2)-Flag.

The Myc-tag sequence was cloned into pCAGGS and named pCAGGS-Myc. The GRP78 cDNA was cloned into pCAGGS-Myc with the restriction enzyme *Not* I using a ClonExpress II One Step Cloning Kit (Vayzme, Nanjing, China).

The mutants of GRP78-Myc were constructed by overlap PCR. For the endoplasmic reticulum DnaJ homolog interaction-defective mutant (R197H), Arg-197 was replaced by His. For ATP binding-defective mutant (G227D), Gly-227 was replaced by Asp. For substrate binding-defective mutant (T4530), Thr-453 was replaced by Asp.

All primer sequences used for the construction of the recombinant plasmids are presented in Table 1. The recombinant plasmids were transfected into PTECs using TransIT-X2® reagent (Mirus Bio, Madison, WI, USA).

4.4 | Recombinant protein expression and purification

The Mhp271 gene was PCR amplified from *M. hyopneumoniae*, the Mhp271 gene lacking the R1-2 region was generated by overlap PCR and the R1-2 region of Mhp271 cDNA was prepared by Comate Biotech Company (Jilin, China). These cDNAs were cloned into the pMAL-c5x vector with the restriction enzymes *Sal* I and *Bam* HI.

The GRP78 gene was PCR amplified from PTECs and cloned into the pGEX-GST vector with the restriction enzymes *Bam* HI and *Sal* I.

These recombinant plasmids were transformed into *E. coli* BL21(DE3) cells. The level of recombinant protein expression was analyzed by SDS-PAGE. Subsequently, the Mhp271-MBP, Mhp271(ΔR1-2)-MBP, and Mhp271 R1-2-MBP fusion proteins were purified by using amylose agarose resin (New England Biolabs) according to the manufacturer's instructions. The prurition of GRP78-GST was performed using Glutathione Sepharose 4 Fast Flow resin (GE Healthcare).

TABLE 1 Primers used in this study

Primer name	Restriction enzyme	Sequence (5′–3′)
GRP78-HA-F	*Kpn* I	GGGGTACCATGAAGCTGTCCCTGGTGG
GRP78-HA-R	*Xho* I	CCGCTCGAGCTACAACTCATCTTTGTCTGCTGAT
GRP78-Myc-F[a]	*Not* I	gatctcgaggctagcgcggccgcATGTGGGCACGGTGGTCG
GRP78-Myc-R[a]	*Not* I	atgagtttttgttctgcggccgcCTACAACTCATCTTTGTCTGCTGATTC
GRP78-GST-F	*Bam* HI	CGGGATCCATGAAGCTGTCCCTGGTGG
GRP78-GST-R	*Sal* I	ACGCGTCGACCAACTCATCTTTGTCTGCTGA
Mhp271-MBP-F[a]	*Sal* I	ggcggccgcgatatcgtcgacATGAGCAAACTGACCAAGAGCA
Mhp271-MBP-R[a]	*Bam* HI	acctgcagggaattcggatccCTTCGCCTGTTTATTTTCTTTTTTG
Mhp271(ΔR1-2)-MBP-F[a]	*Sal* I	ggcggccgcgatatcgtcgacATGGAAGTGTTTGCGGAACTG
Mhp271(ΔR1-2)-MBP-R[a]	*Bam* HI	acctgcagggaattcggatccCTTCGCCTGTTTATTTTCTTTTTTG
Mhp271-Flag-F[a]	*Not* I	gatctcgaggctagcgcggccgcATGAGCAAACTGACCAAGAGCA
Mhp271-Flag-R[a]	*Not* I	atgagtttttgttctgcggccgcCTTCGCCTGTTTATTTTCTTTTTTG
Mhp271a-Flag-F[a]	*Not* I	tacgtctcggcggcggcggccgcATGAGCAAACTGACCAAGAGCA
Mhp271a-Flag-R[a]	*Not* I	tcgtccttgtagtccgcggccgcGTTGAAGTCGGTTTTGGTAATATCTT
Mhp271b-Flag-F[a]	*Not* I	tacgtctcggcggcggcggccgcGAACAGGGCCTGAAAACC
Mhp271b-Flag-R[a]	*Not* I	tcgtccttgtagtccgcggccgcCGCGTCGGTCTTATTCGCC
Mhp271c-Flag-F[a]	*Not* I	tacgtctcggcggcggcggccgcGAAGTGTTTGCGGAACTG
Mhp271c-Flag-R[a]	*Not* I	tcgtccttgtagtccgcggccgcCTTCGCCTGTTTATTTTCTTTTTTG
Mhp271c(ΔR1-1)-Flag-F	*Sac* I	CGAGCTCATGGAAGTGTTTGCGGAACTG AAGCGAAACCAGCAATAGCACCACC
Mhp271c(ΔR1-1)-Flag-R	*Not* I	TGCTATTGCTGGTTTCGCTTTTC TTGCGGCCGCCTTCGCCTGTTTATTTTCTTTTTTGG
Mhp271c(ΔR1-2)-Flag-F	*Sac* I	CGAGCTCATGGAAGTGTTTGCGGAACTG TCCGAAAACCGTAAGCAGCCCAGCG
Mhp271c(ΔR1-2)-Flag-R	*Not I*	GGCTGCTTACGGTTTTCGGAGTTTC TTGCGGCCGCCTTCGCCTGTTTATTTTCTT
Mhp271c(ΔR2)-Flag-F	*Sac* I	CGAGCTCATGGAAGTGTTTGCGGAACTG CCAGAAAAGCGAAGAAAATAGCAAC
Mhp271c(ΔR2)-Flag-R	*Not* I	TATTTTCTTCGCTTTTCTGGCTT TTGCGGCCGCCTTCGCCTGTTTATTTTCTTTTTTG
qPCR[b]	PBD-2-F	ACCTGCTTACGGGTCTTG
	PBD-2-R	CTCTGCTGTGGCTTCTGG

[a]These primers are used in homologous recombination methods to construct recombinant plasmids and homologous arm sequences are denoted by lowercase letters.

[b]The primers are used in quantitative PCR (qPCR). Restriction enzyme sites incorporated into primers are underlined.

The endotoxin concentration of the fusion proteins (<0.04 endotoxin units/ml) was verified using the ToxinSensor chromogenic LAL endotoxin assay kit (GenScript, China).

4.5 | Co-IP assays

HEK293T cells were transfected with the recombinant plasmid GRP78-HA for 36 h and then stimulated by 8 μg/ml *M. hyopneumoniae* LAMPs. The cells were harvested and lysed with the cell lysis buffer (1 protease inhibitor cocktail tablet [Roche]/10 ml NP-40 buffer) for 30 min at 4°C. Supernatants after centrifugation were incubated with anti-HA magnetic beads (Bimake, USA) on an MACSmix Tube rotator at 4°C overnight. The next day, the beads were collected with a magnetic separator (Bimake) and then washed five times to remove the unbound proteins. Proteins bound to the beads were eluted with elution buffer (100 mM glycine-HCl, pH = 3). The eluate was immediately neutralized with 1 M Tris–HCl (pH = 8). Eluted proteins were separated by SDS-PAGE and silver-stained (Beyotime, Nantong, China). The excised gel band was sent to BGI (Beijing, China) and analyzed by MS.

The plasmid expressing GRP78-Myc protein was cotransfected with the plasmids expressing *M. hyopneumoniae* proteins (Mhp271, Mhp271 truncates, or Mhp271 deletions) into HEK293T cells, respectively.

The plasmid expressing Mhp271 R1-2-Flag protein was cotransfected with the GRP78-Myc or the GRP78 mutant plasmids.

At 36 h posttransfection, the cells were lysed with ice-cold lysis buffer for 30 min at 4°C. After centrifugation (8000*g*, 10 min) at 4°C, the clarified extracts were incubated with beads conjugated with anti-Flag (Sigma-Aldrich, USA) or anti-Myc (Sigma-Aldrich, USA) affinity gel on a MACSmix Tube rotator at 4°C overnight. The incubated beads were washed five times with lysis buffer, followed by SDS-PAGE and Western blotting.

4.6 | Cell viability measurements

Cell viability was detected using a Cell Counting Kit-8 (CCK-8) according to the manufacturer's protocol (Vazyme, Nanjing, China).

4.7 | Western blotting

Whole-cell lysates were harvested at the indicated time points. An equal number of cells were lysed with the cell lysis buffer for 30 min at 4°C. The protein concentration was determined using a BCA Protein Assay Kit (Beyotime, Nantong, China). Equal amounts of total cell lysates were separated by SDS-PAGE. The proteins in the gel were transferred onto nitrocellulose membranes (GE Healthcare Life Science, Piscataway, USA), which were then blocked with 5% skim milk in TBST (Solarbio, Beijing, China) at 4°C overnight and then incubated for 2 h with different primary antibodies at room temperature (RT). Antibodies against GRP78 (ab21685) and Myc (ab32) were purchased from Abcam (Cambridge, MA, USA). The antibody against Flag (F7425) was obtained from Sigma-Aldrich (St. Louis, MO, USA). An antibody against β-actin (TA-09) was purchased from Zhongshan Goldenbridge-Bio (Beijing, China). An antibody against MBP was available from New England Biolabs. After washing with TBST, DyLight™ 800-labeled goat antimouse IgG (H + L) or DyLight™ 800-labeled goat antirabbit IgG (H + L) (1:10,000, Kirkegaard & Perry Laboratories, Gaithersburg, USA) was used for detection. The membrane was scanned using an Odyssey infrared imaging system, and the fluorescence intensity of each band was measured using Odyssey 2.1 software (LI-COR Biosciences).

4.8 | Immunofluorescence

HEK293T cells were transfected with GRP78-Myc, Mhp271-Flag, or both and fixed for 30 min in 4% paraformaldehyde (PFA) in PBS. The fixed cells were permeabilized with 0.1% Triton X-100 for 10 min and blocked for 1 h in 0.2% cold-water fish skin gelatin (Sigma). Cells were then incubated with mouse anti-Myc mAb or rabbit anti-Flag polyclonal antibodies for 1 h at RT, washed three times with PBS, and incubated for 1 h with secondary antibodies coupled to Alexa Fluor 633 or Alexa Fluor 488 (Invitrogen). The cell nuclei were labeled with DAPI (1:1000, Sigma). Fluorescence images were acquired using a confocal microscope (Zeiss, LSM800).

4.9 | Real-time quantitative RT-PCR and adherence assessment

Total RNA was extracted from the cells using an RNeasy Mini kit (Qiagen Sciences, Hilden, Germany) according to the manufacturer's instructions. RNA was reverse transcribed using a Transcriptor First-Strand cDNA Synthesis Kit (Roche Diagnostics, Indianapolis, USA).

qPCR was performed in triplicate using FastStart Universal SYBR Green Master Mix (Rox) (Roche Diagnostics, Indianapolis, USA). All data were acquired using a QuantStudio™ 3 real-time PCR system (Applied Biosystems, Carlsbad, USA). The expression value of each gene was normalized to that of GAPDH, and final values were calculated using the ΔΔCt method. The results were analyzed using QuantStudio™ Design & Analysis software v1.4 (Applied Biosystems). The PBD-2 primer sequences used in this study are provided in Table 1.

Adherence assessment was performed as described previously (Pan et al., 2020). Briefly, the *M. hyopneumoniae* copy number was quantitated in cell samples by qPCR using a specific TaqMan probe assay (Wu et al., 2012): the forward primer (F: 5′-CCAGAACCAAATTCCTTCGCTG-3′), reverse primer (R: 5′-ACTGGCTGAACTTCATCTGGGCTA-3′), and TaqMan probe (5′-FAM-AGCAGATCTTAGTCAAAGTGCCCGTG-BHQ-3′). The composition of the qPCR assay mixture was according to the manufacturer's protocol (Premix Ex Taq™ [Probe qPCR], TaKaRa, Dalian, China). Amplification was performed using a QuantStudio™ 3 real-time PCR system (Applied Biosystems, Carlsbad, USA). In each plate, 10-fold dilutions of the standard plasmid (10^{11}–10^{5} copies/μl) and the blank control were included. Each sample was assayed three times.

4.10 | Far-Western blotting

To explore whether *M. hyopneumoniae* Mhp271 or Mhp271 R1-2 could directly bind to GRP78, protein–protein interactions method Far-Western blotting was performed. A total of 1 μg of recombinant proteins (Mhp271-MBP or Mhp271 R1-2-MBP) and a negative control (PDH-MBP or Mhp271(ΔR1-2)-MBP) were separated by SDS-PAGE and transferred onto nitrocellulose membranes. After blocking with 5% (w/v) skimmed milk, the membrane was incubated with 1 μg/ml GRP78-GST or GST protein, followed by incubation with rabbit anti-GRP78 or anti-GST antibody (Abcam) as the primary antibody and DyLight™ 800-labeled goat antirabbit IgG (H + L) (1:10,000 dilution, Kirkegaard & Perry Laboratories) as the secondary antibody. Finally, the membrane was scanned using an Odyssey infrared imaging system.

4.11 | Purifying antibodies against *M. hyopneumoniae* Mhp271

Anti-*M. hyopneumoniae* Mhp271 antibodies were purified from the murine serum anti-Mhp271 as described previously (Piccinni

& Guille, 2020). Three milliliters of antiserum were mixed with 6 ml of 60 mM sodium acetate (pH 4.0), and 100% caprylic acid (for a final concentration of 2.5%) was added while the mixture was stirred. Upon stirring for 20–30 min, the mixture was centrifuged at 5100 g for 20 min, and the supernatant was collected (Total IgG).

One milliliter amylose resin was poured into a 5 ml empty column and washed with five column volumes of Column Buffer (20 mM Tris–HCl, 200 mM NaCl and 1 mM EDTA). The resin was incubated with 5 mg Mhp271-MBP protein for 30 min at room temperature. After washing the column with three column volumes of Column Buffer, the total IgG was passed through the column three times. About 3.5 M potassium thiocyanate was directly added onto the beads to elute the antibody, prior to which the columns were rinsed with 10 volumes of Column Buffer and 0.5 M NaCl-PBS, respectively.

Two-column volumes of 10 mM sodium bicarbonate were passed through a desalting column and the eluted antibody was loaded onto the column. The column was placed in the 50 ml centrifuge tube and centrifuged at 2000 rpm for 5 min. The liquid (purified antibody) at the bottom of the centrifuge tube was collected and the IgG concentration was determined by UV spectroscopy (275 nm).

4.12 | Blocking assay

M. hyopneumoniae cells (1×10^6 CFU/ml) were washed three times with PBS and preincubated with the purified antibodies against Mhp271 (20 and 50 μg/ml) or PBS at 37°C for 30 min. The bacterial suspension in DMEM was added to PTECs.

Mhp271 fusion protein (8 μg/ml) was preincubated with murine serum (diluted 1:20, 1:50, 1:100, and 1:200) against the Mhp271 R1-2 protein at 37°C for 30 min. Mhp271 preincubated with negative murine serum (diluted 1:20) was used as the control. The pretreated Mhp271 fusion protein was added to PTECs.

Following incubation for 12 h, the cells were washed three times with PBS and subjected to Western blotting analysis.

4.13 | Statistical analysis

GraphPad Prism software (version 7.0 for Mac; GraphPad Software Inc.) was used for all statistical analyses. Data obtained from several experiments are reported as the mean ± *SD*. The significance of differences between the two groups was determined with a two-tailed Student's *t* test. One-way analysis of variances (ANOVA) with Dunnett's or Tukey's test was employed for multigroup comparisons. For all analyses, a probability (p) value of $< .05$ was considered statistically significant.

AUTHORS' CONTRIBUTION

The manuscript was written by Q.P.; experiments and data analysis were performed by Q.P., Q.X., T.L., and Y.Z.; and the study was designed by Q.P., Q.X., and J.X.

CONFLICT OF INTEREST

The authors declare that they have no conflicts of interest. The corresponding author had full access to all the data and accepts the final responsibility for the decision to submit this manuscript for publication.

DATA AVAILABILITY STATEMENT

The data that support the findings of this study are available from the corresponding author upon reasonable request.

ETHICS STATEMENT

Primary porcine tracheal epithelial cells (PTECs) collection was approved by the Committee on the Ethics of Animal Experiments of the Harbin Veterinary Research Institute of the Chinese Academy of Agricultural Sciences and performed according to the approved animal care guidelines and protocols.

ORCID

Qiao Pan https://orcid.org/0000-0001-8023-6109

REFERENCES

Adams, C., Pitzer, J. & Minion, F.C. (2005) In vivo expression analysis of the P97 and P102 paralog families of mycoplasma hyopneumoniae. *Infection and Immunity*, *73*(11), 7784–7787.

Alshareef, M.H., Hartland, E.L. & McCaffrey, K. (2021) Effectors targeting the unfolded protein response during intracellular bacterial infection. *Microorganisms*, *9*(4), 705.

Apweiler, R., Attwood, T.K., Bairoch, A., Bateman, A., Birney, E., Biswas, M. et al. (2001) The InterPro database, an integrated documentation resource for protein families, domains and functional sites. *Nucleic Acids Research*, *29*(1), 37–40.

Ball, L.J., Kühne, R., Schneider-Mergener, J. & Oschkinat, H. (2005) Recognition of proline-rich motifs by protein–protein-interaction domains. *Angewandte Chemie International Edition*, *44*(19), 2852–2869.

Bellani, S., Mescola, A., Ronzitti, G., Tsushima, H., Tilve, S., Canale, C. et al. (2014) GRP78 clustering at the cell surface of neurons transduces the action of exogenous alpha-synuclein. *Cell Death & Differentiation*, *21*(12), 1971–1983.

Berry, I.J., Jarocki, V.M., Tacchi, J.L., Raymond, B.B., Widjaja, M., Padula, M.P. et al. (2017) N-terminomics identifies widespread endoproteolysis and novel methionine excision in a genome-reduced bacterial pathogen. *Scientific Reports*, *7*(1), 1–17.

Bhattacharjee, G., Ahamed, J., Pedersen, B., El-Sheikh, A., Mackman, N., Ruf, W. et al. (2005) Regulation of tissue factor–mediated initiation of the coagulation cascade by cell surface grp78. *Arteriosclerosis, Thrombosis, and Vascular Biology*, *25*(8), 1737–1743.

Bogema, D.R., Deutscher, A.T., Woolley, L.K., Seymour, L.M., Raymond, B.B., Tacchi, J.L. et al. (2012) Characterization of cleavage events in the multifunctional cilium adhesin Mhp684 (P146) reveals a mechanism by which mycoplasma hyopneumoniae regulates surface topography. *mBio*, *3*(2), e00282-00211.

Bogema, D.R., Scott, N.E., Padula, M.P., Tacchi, J.L., Raymond, B.B., Jenkins, C. et al. (2011) Sequence TTKF↓ QE defines the site of proteolytic cleavage in Mhp683 protein, a novel glycosaminoglycan and cilium adhesin of mycoplasma hyopneumoniae. *Journal of Biological Chemistry*, *286*(48), 41217–41229.

Boguslavsky, S., Menaker, D., Lysnyansky, I., Liu, T., Levisohn, S., Rosengarten, R. et al. (2000) Molecular characterization of the

mycoplasma gallisepticum pvpA gene which encodes a putative variable cytadhesin protein. *Infection and Immunity*, *68*(7), 3956–3964.

Broquet, A.H., Lenoir, C., Gardet, A., Sapin, C., Chwetzoff, S., Jouniaux, A.-M. et al. (2007) Hsp70 negatively controls rotavirus protein bioavailability in caco-2 cells infected by the rotavirus RF strain. *Journal of Virology*, *81*(3), 1297–1304.

Burnett, T.A., Dinkla, K., Rohde, M., Chhatwal, G.S., Uphoff, C., Srivastava, M. et al. (2006) P159 is a proteolytically processed, surface adhesin of mycoplasma hyopneumoniae: defined domains of P159 bind heparin and promote adherence to eukaryote cells. *Molecular Microbiology*, *60*(3), 669–686.

Celli, J. & Tsolis, R.M. (2015) Bacteria, the endoplasmic reticulum and the unfolded protein response: friends or foes? *Nature Reviews Microbiology*, *13*(2), 71–82.

Chen, Y.-J., Chen, Y.-H., Chow, L.-P., Tsai, Y.-H., Chen, P.-H., Huang, C.--Y.F. et al. (2010) Heat shock protein 72 is associated with the hepatitis C virus replicase complex and enhances viral RNA replication. *Journal of Biological Chemistry*, *285*(36), 28183–28190.

Chengcheng, Z., Fuxi, Z., Mengjiao, G., Baoyang, R., Xuefeng, W., Yantao, W. et al. (2020) CSFV protein NS5A activates the unfolded protein response to promote viral replication. *Virology*, *541*, 75–84.

Chu, H., Chan, C.-M., Zhang, X., Wang, Y., Yuan, S., Zhou, J. et al. (2018) Middle East respiratory syndrome coronavirus and bat coronavirus HKU9 both can utilize GRP78 for attachment onto host cells. *Journal of Biological Chemistry*, *293*(30), 11709–11726.

Clampitt, J.M., Madsen, M.L. & Minion, F.C. (2021) Construction of mycoplasma hyopneumoniae P97 null mutants. *Frontiers in Microbiology*, *12*, 950.

Cytryńska, M., Rahnamaeian, M., Zdybicka-Barabas, A., Dobslaff, K., Zuechner, T., Sacheau, G. et al. (2020) Proline-rich antimicrobial peptides in medicinal maggots of Lucilia sericata interact with bacterial DnaK but do not inhibit protein synthesis. *Frontiers in Pharmacology*, *11*, 532.

Dallo, S., Lazzell, A., Chavoya, A., Reddy, S. & Baseman, J. (1996) Biofunctional domains of the mycoplasma pneumoniae P30 adhesin. *Infection and Immunity*, *64*(7), 2595–2601.

Deutscher, A.T., Jenkins, C., Minion, F.C., Seymour, L.M., Padula, M.P., Dixon, N.E. et al. (2010) Repeat regions R1 and R2 in the P97 paralogue Mhp271 of mycoplasma hyopneumoniae bind heparin, fibronectin and porcine cilia. *Molecular Microbiology*, *78*(2), 444–458.

Deutscher, A.T., Tacchi, J.L., Minion, F.C., Padula, M.P., Crossett, B., Bogema, D.R. et al. (2012) Mycoplasma hyopneumoniae surface proteins Mhp385 and Mhp384 bind host cilia and glycosaminoglycans and are endoproteolytically processed by proteases that recognize different cleavage motifs. *Journal of Proteome Research*, *11*(3), 1924–1936.

Elfiky, A.A. (2020) Ebola virus glycoprotein GP1—host cell-surface HSPA5 binding site prediction. *Cell Stress and Chaperones*, *25*(3), 541–548.

Gonzalez-Gronow, M., Selim, M.A., Papalas, J. & Pizzo, S.V. (2009) GRP78: a multifunctional receptor on the cell surface. *Antioxidants & Redox Signaling*, *11*(9), 2299–2306.

Guex, N. & Peitsch, M.C. (1997) SWISS-MODEL and the Swiss-Pdb viewer: an environment for comparative protein modeling. *Electrophoresis*, *18*(15), 2714–2723.

Hannan, A.J. (2018) Tandem repeats mediating genetic plasticity in health and disease. *Nature Reviews Genetics*, *19*(5), 286–298.

He, J., You, X., Zeng, Y., Yu, M., Zuo, L. & Wu, Y. (2009) Mycoplasma genitalium-derived lipid-associated membrane proteins activate NF-κB through toll-like receptors 1, 2, and 6 and CD14 in a MyD88-dependent pathway. *Clinical and Vaccine Immunology*, *16*(12), 1750–1757.

Hetz, C., Chevet, E. & Oakes, S.A. (2015) Proteostasis control by the unfolded protein response. *Nature Cell Biology*, *17*(7), 829–838.

Hirayama, E., Atagi, H., Hiraki, A. & Kim, J. (2004) Heat shock protein 70 is related to thermal inhibition of nuclear export of the influenza virus ribonucleoprotein complex. *Journal of Virology*, *78*(3), 1263–1270.

Honda, T., Horie, M., Daito, T., Ikuta, K. & Tomonaga, K. (2009) Molecular chaperone BiP interacts with Borna disease virus glycoprotein at the cell surface. *Journal of Virology*, *83*(23), 12622–12625.

Hotamisligil, G.S. (2010) Endoplasmic reticulum stress and the inflammatory basis of metabolic disease. *Cell*, *140*(6), 900–917.

Hsu, T., Artiushin, S. & Minion, F.C. (1997) Cloning and functional analysis of the P97 swine cilium adhesin gene of mycoplasma hyopneumoniae. *Journal of Bacteriology*, *179*(4), 1317–1323.

Hsu, T. & Minion, F.C. (1998) Identification of the cilium binding epitope of theMycoplasma hyopneumoniae P97 Adhesin. *Infection and Immunity*, *66*(10), 4762–4766.

Ibrahim, I.M., Abdelmalek, D.H. & Elfiky, A.A. (2019) GRP78: A cell's response to stress. *Life Sciences*, *226*, 156–163.

Iordanskiy, S., Zhao, Y., Dubrovsky, L., Iordanskaya, T., Chen, M., Liang, D. et al. (2004) Heat shock protein 70 protects cells from cell cycle arrest and apoptosis induced by human immunodeficiency virus type 1 viral protein R. *Journal of Virology*, *78*(18), 9697–9704.

Jarocki, V.M., Raymond, B.B.A., Tacchi, J.L., Padula, M.P. & Djordjevic, S.P. (2019) Mycoplasma hyopneumoniae surface-associated proteases cleave bradykinin, substance P, neurokinin a and neuropeptide Y. *Scientific Reports*, *9*(1), 1–12.

Jenkins, C., Wilton, J.L., Minion, F.C., Falconer, L., Walker, M.J. & Djordjevic, S.P. (2006) Two domains within the mycoplasma hyopneumoniae cilium adhesin bind heparin. *Infection and Immunity*, *74*(1), 481–487.

Jindadamrongwech, S., Thepparit, C. & Smith, D. (2004) Identification of GRP 78 (BiP) as a liver cell expressed receptor element for dengue virus serotype 2. *Archives of Virology*, *149*(5), 915–927.

de Jong, M.F., Starr, T., Winter, M.G., den Hartigh, A.B., Child, R., Knodler, L.A. et al. (2013) Sensing of bacterial type IV secretion via the unfolded protein response. *MBio*, *4*(1), e00418-00412.

Kampinga, H.H. & Craig, E.A. (2010) The HSP70 chaperone machinery: J proteins as drivers of functional specificity. *Nature Reviews Molecular Cell Biology*, *11*(8), 579–592.

Kirchner, M. & Meyer, T.F. (2005) The PilC adhesin of the Neisseria type IV pilus–binding specificities and new insights into the nature of the host cell receptor. *Molecular Microbiology*, *56*(4), 945–957.

Le Carrou, J., Laurentie, M., Kobisch, M. & Gautier-Bouchardon, A. (2006) Persistence of mycoplasma hyopneumoniae in experimentally infected pigs after marbofloxacin treatment and detection of mutations in the parC gene. *Antimicrobial Agents and Chemotherapy*, *50*(6), 1959–1966.

Leal Zimmer, F.M., Paes, J.A., Zaha, A. & Ferreira, H.B. (2020) Pathogenicity & virulence of mycoplasma hyopneumoniae. *Virulence*, *11*(1), 1600–1622.

Lee, A.S. (2014) Glucose-regulated proteins in cancer: molecular mechanisms and therapeutic potential. *Nature Reviews Cancer*, *14*(4), 263–276.

Li, G., Zhang, J., Tong, X., Liu, W. & Ye, X. (2011) Heat shock protein 70 inhibits the activity of influenza a virus ribonucleoprotein and blocks the replication of virus in vitro and in vivo. *PLoS One*, *6*(2), e16546.

Liu, M., Spellberg, B., Phan, Q.T., Fu, Y., Fu, Y., Lee, A.S. et al. (2010) The endothelial cell receptor GRP78 is required for mucormycosis pathogenesis in diabetic mice. *The Journal of Clinical Investigation*, *120*(6), 1914–1924.

Maes, D., Boyen, F., Devriendt, B., Kuhnert, P., Summerfield, A. & Haesebrouck, F. (2021) Perspectives for improvement of mycoplasma hyopneumoniae vaccines in pigs. *Veterinary Research*, *52*(1), 1–20.

Maes, D., Sibila, M., Kuhnert, P., Segalés, J., Haesebrouck, F. & Pieters, M. (2018) Update on mycoplasma hyopneumoniae infections in pigs: knowledge gaps for improved disease control. *Transboundary and Emerging Diseases*, *65*, 110–124.

Maes, D., Sibila, M. & Pieters, M. (2021) Mycoplasmas in swine. CABI.

Martines, R.B., Ng, D.L., Greer, P.W., Rollin, P.E. & Zaki, S.R. (2015) Tissue and cellular tropism, pathology and pathogenesis of Ebola and Marburg viruses. *The Journal of Pathology*, *235*(2), 153–174.

Minion, F.C., Adams, C. & Hsu, T. (2000) R1 region of P97 mediates adherence of mycoplasma hyopneumoniae to swine cilia. *Infection and Immunity*, *68*(5), 3056–3060.

Mori, K. (2000) Tripartite management of unfolded proteins in the endoplasmic reticulum. *Cell*, *101*(5), 451–454.

Morinaga, N., Yahiro, K., Matsuura, G., Moss, J. & Noda, M. (2008) Subtilase cytotoxin, produced by Shiga-toxigenic Escherichia coli, transiently inhibits protein synthesis of Vero cells via degradation of BiP and induces cell cycle arrest at G1 by downregulation of cyclin D1. *Cellular Microbiology*, *10*(4), 921–929.

Murakami, J., Terao, Y., Morisaki, I., Hamada, S. & Kawabata, S. (2012) Group a streptococcus adheres to pharyngeal epithelial cells with salivary proline-rich proteins via GrpE chaperone protein. *Journal of Biological Chemistry*, *287*(26), 22266–22275.

Nain, M., Mukherjee, S., Karmakar, S.P., Paton, A.W., Paton, J.C., Abdin, M. et al. (2017) GRP78 is an important host factor for Japanese encephalitis virus entry and replication in mammalian cells. *Journal of Virology*, *91*(6), e02274-02216.

Niwa, H., Yamamura, K. & Miyazaki, J. (1991) Efficient selection for high-expression transfectants with a novel eukaryotic vector. *Gene*, *108*(2), 193–199.

Padwad, Y., Mishra, K., Jain, M., Chanda, S. & Ganju, L. (2010) Dengue virus infection activates cellular chaperone Hsp70 in THP-1 cells: downregulation of Hsp70 by siRNA revealed decreased viral replication. *Viral Immunology*, *23*(6), 557–565.

Pan, Q., Wang, X., Liu, T., Yu, Y., Li, L., Zhou, R. et al. (2020) Mycoplasma hyopneumoniae inhibits porcine beta-defensin 2 production by blocking the unfolded protein response to facilitate epithelial adhesion and infection. *Infection and Immunity*, *88*(7), e00164-00120.

Paton, A.W., Beddoe, T., Thorpe, C.M., Whisstock, J.C., Wilce, M.C., Rossjohn, J. et al. (2006) AB 5 subtilase cytotoxin inactivates the endoplasmic reticulum chaperone BiP. *Nature*, *443*(7111), 548–552.

Pavio, N., Romano, P.R., Graczyk, T.M., Feinstone, S.M. & Taylor, D.R. (2003) Protein synthesis and endoplasmic reticulum stress can be modulated by the hepatitis C virus envelope protein E2 through the eukaryotic initiation factor 2α kinase PERK. *Journal of Virology*, *77*(6), 3578–3585.

Pfaffenbach, K.T. & Lee, A.S. (2011) The critical role of GRP78 in physiologic and pathologic stress. *Current Opinion in Cell Biology*, *23*(2), 150–156.

Philippova, M., Ivanov, D., Joshi, M.B., Kyriakakis, E., Rupp, K., Afonyushkin, T. et al. (2008) Identification of proteins associating with glycosylphosphatidylinositol-anchored T-cadherin on the surface of vascular endothelial cells: role for Grp78/BiP in T-cadherin-dependent cell survival. *Molecular and Cellular Biology*, *28*(12), 4004–4017.

Piccinni, M.Z. & Guille, M.J. (2020) Purifying antibodies raised against Xenopus peptides. *Cold Spring Harbor Protocols*, *2020*(9) pdb.prot105619.

Pierce, B.G., Wiehe, K., Hwang, H., Kim, B.-H., Vreven, T. & Weng, Z. (2014) ZDOCK server: interactive docking prediction of protein–protein complexes and symmetric multimers. *Bioinformatics*, *30*(12), 1771–1773.

Raymond, B., Madhkoor, R., Schleicher, I., Uphoff, C.C., Turnbull, L., Whitchurch, C.B. et al. (2018a) Extracellular actin is a receptor for mycoplasma hyopneumoniae. *Frontiers in Cellular and Infection Microbiology*, *8*, 54.

Raymond, B., Turnbull, L., Jenkins, C., Madhkoor, R., Schleicher, I., Uphoff, C. et al. (2018b) Mycoplasma hyopneumoniae resides intracellularly within porcine epithelial cells. *Scientific Reports*, *8*(1), 1–13.

Schultz, J., Milpetz, F., Bork, P. & Ponting, C.P. (1998) SMART, a simple modular architecture research tool: identification of signaling domains. *Proceedings of the National Academy of Sciences*, *95*(11), 5857–5864.

Seymour, L.M., Jenkins, C., Deutscher, A.T., Raymond, B.B., Padula, M.P., Tacchi, J.L. et al. (2012) Mhp182 (P102) binds fibronectin and contributes to the recruitment of plasmin (ogen) to the mycoplasma hyopneumoniae cell surface. *Cellular Microbiology*, *14*(1), 81–94.

Shimizu, T., Kida, Y. & Kuwano, K. (2005) A dipalmitoylated lipoprotein from mycoplasma pneumoniae activates NF-κB through TLR1, TLR2, and TLR6. *The Journal of Immunology*, *175*(7), 4641–4646.

Surtees, R., Dowall, S.D., Shaw, A., Armstrong, S., Hewson, R., Carroll, M.W. et al. (2016) Heat shock protein 70 family members interact with Crimean-Congo hemorrhagic fever virus and Hazara virus nucleocapsid proteins and perform a functional role in the nairovirus replication cycle. *Journal of Virology*, *90*(20), 9305–9316.

Taguwa, S., Maringer, K., Li, X., Bernal-Rubio, D., Rauch, J.N., Gestwicki, J.E. et al. (2015) Defining Hsp70 subnetworks in dengue virus replication reveals key vulnerability in flavivirus infection. *Cell*, *163*(5), 1108–1123.

Tardif, K.D., Mori, K., Kaufman, R.J. & Siddiqui, A. (2004) Hepatitis C virus suppresses the IRE1-XBP1 pathway of the unfolded protein response. *Journal of Biological Chemistry*, *279*(17), 17158–17164.

Triantafilou, K., Fradelizi, D., Wilson, K. & Triantafilou, M. (2002) GRP78, a coreceptor for coxsackievirus A9, interacts with major histocompatibility complex class I molecules which mediate virus internalization. *Journal of Virology*, *76*(2), 633–643.

Tsai, Y.-L., Zhang, Y., Tseng, C.-C., Stanciauskas, R., Pinaud, F. & Lee, A.S. (2015) Characterization and mechanism of stress-induced translocation of 78-kilodalton glucose-regulated protein (GRP78) to the cell surface. *Journal of Biological Chemistry*, *290*(13), 8049–8064.

Vakser, I.A. (2014) Protein-protein docking: from interaction to interactome. *Biophysical Journal*, *107*(8), 1785–1793.

Vogl, G., Plaickner, A., Szathmary, S., Stipkovits, L., Rosengarten, R. & Szostak, M.P. (2008) Mycoplasma gallisepticum invades chicken erythrocytes during infection. *Infection and Immunity*, *76*(1), 71–77.

Wang, H., He, L., Liu, B., Feng, Y., Zhou, H., Zhang, Z. et al. (2018) Establishment and comparison of air-liquid interface culture systems for primary and immortalized swine tracheal epithelial cells. *BMC Cell Biology*, *19*(1), 1–10.

Wang, J., Lee, J., Liem, D. & Ping, P. (2017) HSPA5 gene encoding Hsp70 chaperone BiP in the endoplasmic reticulum. *Gene*, *618*, 14–23.

Wilton, J., Jenkins, C., Cordwell, S.J., Falconer, L., Minion, F.C., Oneal, D.C. et al. (2009) Mhp493 (P216) is a proteolytically processed, cilium and heparin binding protein of mycoplasma hyopneumoniae. *Molecular Microbiology*, *71*(3), 566–582.

Wu, Y., Jin, M., Bai, F., Zhang, X., Hua, L., Lei, Z. et al. (2012) Development and application of TaqMan-BHQ real time PCR assay for detection of mycoplasma hyopneumoniae P97. *Chinese Veterinary Science/Zhongguo Shouyi Kexue*, *42*(12), 1268–1272.

Zhang, Y. (2008) I-TASSER server for protein 3D structure prediction. *BMC Bioinformatics*, *9*(1), 1–8.

Zhu, G. & Lee, A.S. (2015) Role of the unfolded protein response, GRP78 and GRP94 in organ homeostasis. *Journal of Cellular Physiology*, *230*(7), 1413–1420.

SUPPORTING INFORMATION

Additional supporting information can be found online in the Supporting Information section at the end of this article.

How to cite this article: Pan, Q., Xu, Q., Liu, T., Zhang, Y. & Xin, J. (2022). *Mycoplasma hyopneumoniae* membrane protein Mhp271 interacts with host UPR protein GRP78 to facilitate infection. *Molecular Microbiology*, *118*, 208–222. https://doi.org/10.1111/mmi.14963